Translational Energy Dependence and Potential Energy Surfaces of Gas Phase S_N2 and Addition−Elimination Reactions

Stephen L. Craig, Meili Zhong, and John I. Brauman*

Contribution from the Department of Chemistry, Stanford University, Stanford, California 94305-5080

Received February 22, 1999

Abstract: The translational energy dependence of several gas-phase S_N2 and carbonyl addition−elimination reaction rate constants has been measured in an FT-ICR. The relative energy dependences of the reactions are qualitatively consistent with variations in the reaction potential surfaces that are inferred from their thermal rate constants, which comprise a wide range of reaction efficiencies. Furthermore, the observed energy dependence of each reaction agrees quantitatively with RRKM calculations of the reaction rate constants. We conclude that, although nonstatistical dynamics are observed in some S_N2 reactions, statistical reaction rate theory is, in general, an accurate means of interpreting the translational energy dependence of bimolecular ion−molecule reaction rate constants.

The kinetics of gas-phase bimolecular ion−molecule reactions are generally interpreted with some form of unimolecular statistical reaction rate theory, such as phase space theory (PST) or Rice−Ramsperger−Kassel−Marcus (RRKM) theory.[1−5] Ion−molecule reactions are seemingly well-suited for a unimolecular treatment, because the association energies are large and intermediate complexes are expected to be long-lived. It therefore seems reasonable to assume that energy is redistributed statistically within the bimolecular collision complex and that the kinetics would be accurately described by unimolecular reaction rate theory.

Recent experimental and theoretical studies of gas-phase S_N2 reactions, however, suggest that the assumption of statistical behavior in ion−molecule intermediate complexes is not valid for at least some members of this important class of reactions.[6−25]

This "nonstatistical" behavior has been documented for several halide−methyl halide reactions, especially those in eq 1, and a thorough discussion of recent work in the area is given by Hase.[20]

$$X^- + CH_3Y \rightarrow Y^- + CH_3X \quad (1)$$
$$\text{a: } X = Cl; Y = Cl$$
$$\text{b: } X = Cl; Y = Br$$
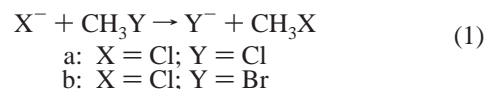
Trajectory calculations by Vande Linde and Hase on eq 1a show that some reactions occur through a direct mechanism, bypassing formation of an intermediate metastable complex,[8] and energy in the neutral carbon−chlorine stretch greatly enhances the probability of direct chloride exchange. Further, in complexes that do not react directly, the calculated rate of unimolecular dissociation is an order of magnitude greater than the statistical value.[10] This value has recently been confirmed experimentally.[26] The behavior of the collision complex in eq 1a is not statistical, and an accurate interpretation of the kinetics of that reaction requires an understanding of the detailed dynamics of individual collision events.

The related reaction 1b also displays nonstatistical characteristics. The translational and internal energy dependences of 1b have been measured in a variable temperature selected ion flow drift tube (VT-SIFDT) by Viggiano et al.,[16] who found that the rate constant depends differently on energy in the reactant translational and vibrational degrees of freedom. While the disparate responses to these two initial energy distributions strongly suggest nonstatistical behavior, the effective potential energy surface of the reaction changes with increased angular momentum at higher reactant collision energies. Translational

(1) Marcus, R. A. *J. Chem. Phys.* **1952,** *20,* 359.

(2) Marcus, R. A.; Hase, W. L.; Swamy, K. N. *J. Phys. Chem.* **1984,** *88,* 6717.

(3) Robinson, P. J.; Holbrook, K. A. *Unimolecular Reactions*; Interscience: London, 1972.

(4) Forst, W. *Theory of Unimolecular Reactions*; Academic Press: New York, 1973.

(5) Gilbert, R. G.; Smith, S. C. *Theory of Unimolecular and Recombination Reactions*; Blackwells Scientific: Oxford, 1990.

(6) Basilevsky, M. V.; Ryaboy, V. M. *Chem. Phys. Lett.* **1986,** *129,* 71.

(7) Ryaboy, V. M. *Chem. Phys. Lett.* **1989,** *159,* 371.

(8) Vande Linde, S. R.; Hase, W. L. *J. Am. Chem. Soc.* **1989,** *111,* 2349−2351.

(9) Vande Linde, S. R.; Hase, W. L. *J. Phys. Chem.* **1990,** *94,* 6148−6150.

(10) Vande Linde, S. R.; Hase, W. L. *J. Chem. Phys.* **1990,** *93,* 7962.

(11) Vande Linde, S. R.; Hase, W. L. *J. Phys. Chem.* **1990,** *94,* 2778−2788.

(12) Cho, Y. J.; Vande Linde, S. R.; Zhu, L.; Hase, W. L. *J. Chem. Phys.* **1992,** *96,* 8275.

(13) Graul, S. T.; Bowers, M. T. *J. Am. Chem. Soc.* **1991,** *113,* 9696−9697.

(14) Graul, S.; Bowers, M. T. *J. Am. Chem. Soc.* **1994,** *116,* 3875.

(15) Graul, S. T.; Carpenter, C. J.; Bushnell, J. E.; van Koppen, P. A. M.; Bowers, M. T. *J. Am. Chem. Soc.* **1998,** *120,* 6785−6796.

(16) Viggiano, A. A.; Morris, R. A.; Paschkewitz, J. S.; Paulson, J. F. *J. Am. Chem. Soc.* **1992,** *114,* 10477.

(17) Viggiano, A. A.; Morris, R. A. *J. Phys. Chem.* **1996,** *100,* 19227−19240.

(18) Wang, H.; Peslherbe, G. H.; Hase, W. L. *J. Am. Chem. Soc.* **1994,** *116,* 9644.

(19) Wang, H.; Hase, W. L. *J. Am. Chem. Soc.* **1995,** *117,* 9347−9356.

(20) Hase, W. L. *Science* **1994,** *266,* 998−1002.

(21) Hu, W.-P.; Truhlar, D. G. *J. Am. Chem. Soc.* **1995,** *117,* 10726−10734.

(22) Wang, H.; Goldfield, E. M.; Hase, W. L. *J. Chem. Soc., Faraday Trans.* **1997,** *93,* 737−746.

(23) Chabinyc, M. L.; Craig, S. L.; Regan, C. K.; Brauman, J. I. *Science* **1998,** *279,* 1882−1886.

(24) DeTuri, V. F.; Hintz, P. A.; Ervin, K. M. *J. Phys. Chem. A* **1997,** *101,* 5969−5986.

(25) Mann, D. J.; Hase, W. L. *J. Phys. Chem. A* **1998,** *102,* 6208−6214.

(26) Li, C.; Ross, P.; Szulejko, J. E.; McMahon, T. B. *J. Am. Chem. Soc.* **1996,** *118,* 9360−9367.

and vibrational energy, therefore, should have different effects on the observed rate constant. The rate constant of eq 1b, however, falls off much more rapidly with kinetic energy than expected based on a rigorous statistical model.[19]

Complementary evidence for nonstatistical behavior in eq 1b was provided by Graul and Bowers, who reported the kinetic energy release distribution (KERD), or relative translational energy of the bromide and methyl chloride products, from the decomposition of metastable chloride−methyl bromide reactant complexes in eq 1b.[13] The experimentally observed KERD is significantly lower than that predicted by statistical phase space theory, revealing that the energy generated in the exothermic reaction was trapped in the vibrational modes of the neutral molecule rather than distributed statistically between vibrational and translational modes. Further work by the same authors demonstrated that this result is true not only for eq 1b, but also for a series of S$_N$2 reactions.[14,15]

More recently, work in our laboratory has revealed nonstatistical dynamics in a highly energetic S$_N$2 intermediate.[27] The intermediate reactant complex [Cl·CH$_3$OC(O)CF$_3$]$^-$ was generated with approximately 55 kcal mol^{-1} of internal energy from an exothermic carbonyl exchange reaction. When generated in this manner, the intermediate was at least four times as likely to react than the expectation based on statistical theory; there is unquestionably a dynamic bias toward energy going into the S$_N$2 reaction coordinate relative to the ion−molecule dissociation channel.

Taken together, the trajectory calculations, kinetic energy dependence work, and KERD studies present a self-consistent picture of nonstatistical dynamics in these simple gas-phase S$_N$2 reactions. Energy is either unable to find its way from vibrational degrees of freedom to relative translational degrees of freedom (KERD experiments) or from translational modes to vibrational (trajectory calculations and kinetic energy dependence). The S$_N$2 reactions exhibit a bottleneck to T ↔ V energy transfer, between modes to which Hase refers as "intermolecular" (T) and "intramolecular" (V) degrees of freedom.[20]

The implications of these results are potentially far-reaching, because the intermolecular and intramolecular regions of phase space are closely associated with the competing processes that determine reactivity in ion−molecule systems−dissociation and reaction, respectively. Nonstatistical dynamics, if common to the complexes formed in bimolecular ion−molecule reactions, would preclude the use of unimolecular reaction rate theory to interpret the kinetics of these reactions, especially those in which the energy is initially partitioned unevenly. It is therefore of great interest to determine for which systems and in which energy regimes the assumptions of rapid energy redistribution are valid. Recent studies, for example, show that for the S$_N$2 reaction in eq 2, which involves slightly larger reactants than those in eq 1, the rate constant varies with temperature and reactant translational energy in a manner that is quantitatively consistent with statistical calculations.[28,29] These results suggest that the nonstatistical dynamics of eqs 1 at energies not far from room temperature are not general to either ion−molecule or S$_N$2 reactions, and that eqs 1 may in fact be very special cases. A likely reason for nonstatistical behavior in eqs 1 is the lifetimes of the intermediates, which are much shorter[26] (10−100 ps) than the majority of ion−molecule reactions to which
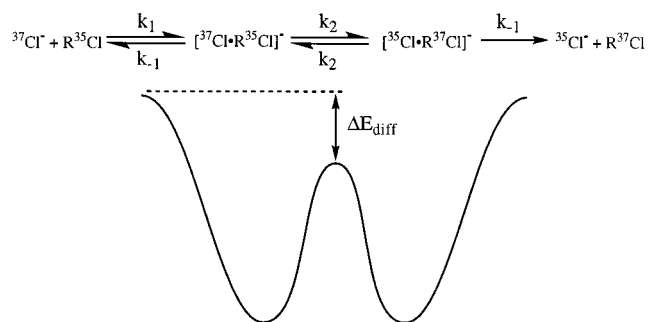
Figure 1. Generalized double-well potential energy surface for the reactions in eqs 2−4. The activation energy, ΔE_{diff}, is inferred from the bimolecular reactivity observed in single-collision events at 350 K. The overall rate of the reaction is a function of the collision rate constant k_1 and the unimolecular rate constants for dissociation (k_{-1}) and S$_N$2 chloride exchange (k_2) of the intermediate collision complex. See text for details.

statistical theories are routinely applied. It is reasonable to expect that, like eq 2, the kinetics of most ion−molecule reactions will be amenable to a statistical interpretation.

$$^{37}\text{Cl}^- + {}^{35}\text{ClCH}_2\text{CN} \rightarrow {}^{35}\text{Cl}^- + {}^{35}\text{ClCH}_2\text{CN} \qquad (2)$$
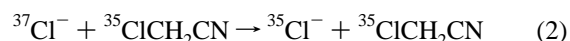
In this study, we test the generality of our previous work on eq 2 by extending it to another gas-phase S$_N$2 and several carbonyl addition−elimination (AE) chloride exchange reactions, eqs 3 and 4, respectively. The potential energy surfaces of these reactions are believed to be quite similar, having the form of a double well (Figure 1).[13,30−35] These reactions are chosen because they comprise a large range of reaction efficiencies ($0.008 < \Phi < 0.38$) and activation energies (-2.6 kcal mol$^{-1} > \Delta E_{\text{diff}} > -11.0$ kcal mol^{-1}, ΔE_{diff} defined in Figure 1).

$$^{37}\text{Cl}^- + m\text{-FC}_6\text{H}_4\text{CH}_2{}^{35}\text{Cl} \rightarrow {}^{35}\text{Cl}^- + m\text{-FC}_6\text{H}_4\text{CH}_2{}^{37}\text{Cl} \quad (3)$$

$$^{37}\text{Cl}^- + \mathbf{R}\text{C}_6\text{H}_4\text{C(O)}{}^{35}\text{Cl} \rightarrow {}^{35}\text{Cl}^- + \mathbf{R}\text{C}_6\text{H}_4\text{C(O)}{}^{37}\text{Cl} \quad (4)$$
$$\mathbf{R} = m\text{-F},\ m\text{-CF}_3,\ \text{H},\ m\text{-CH}_3,\ p\text{-CH}_3$$

Studying a series of similar reactions allows us to evaluate energy redistribution in two ways: by studying both the relative and the absolute kinetic energy dependences of the reactions. If the kinetic energy is distributed statistically in the bimolecular collision complex, the relative kinetic energy dependences of the reactions in eqs 3 and 4 should reflect the variations in their potential energy surfaces. Alternatively, if energy redistribution is inefficient, the kinetic energy dependences will instead reflect the relative efficiency of energy transfer. In addition, the absolute KE dependences also reflect the dynamics of energy transfer. Poor energy exchange should result in absolute kinetic energy dependences that, like that of eq 1b, are more negative than expected from a statistical model.

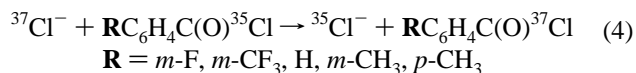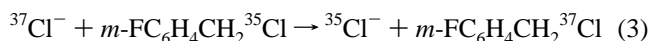(27) Craig, S. L.; Zhong, M.; Brauman, J. I. *J. Am. Chem. Soc.* **1998**, *120*, 12125−12126.

(28) Viggiano, A. A.; Morris, R. A.; Su, T.; Wladkowski, B. D.; Craig, S. L.; Zhong, M.; Brauman, J. I. *J. Am. Chem. Soc.* **1994**, *116*, 2213−2214.

(29) Craig, S. L.; Brauman, J. I. *Science* **1997**, *276*, 1536−1538.

(30) Wilbur, J. L.; Brauman, J. I. *J. Am. Chem. Soc.* **1991**, *113*, 9699−9701.

(31) Wilbur, J. L.; Brauman, J. I. *J. Am. Chem. Soc.* **1994**, *116*, 5839−5846.

(32) Wilbur, J. L.; Brauman, J. I. *J. Am. Chem. Soc.* **1994**, *116*, 9216−9221.

(33) Wladkowski, B. D.; Wilbur, J. L.; Brauman, J. I. *J. Am. Chem. Soc.* **1994**, *116*, 2471−2480.

(34) Cyr, D. M.; Posey, L. A.; Bishea, G. A.; Han, C.-C.; Johnson, M. A. *J. Am. Chem. Soc.* **1991**, *113*, 9697−9699.

(35) Zhong, M.; Brauman, J. I. *J. Am. Chem. Soc.* **1999**, *121*, 2508−2515.

Experimental Section

Experiments were conducted in an IonSpec OMEGA FTMS Fourier transform ion cyclotron resonance spectrometer (FT-ICR) equipped with a 2 in. cubic stainless steel cell and an electromagnet operating at 6.0 kG.[36,37] Background pressure in the vacuum chamber containing the FT-ICR cell was typically 3×10^{-9} Torr. All chemicals were purchased from Aldrich and distilled prior to use, then subjected to multiple freeze−pump−thaw cycles prior to introduction into the vacuum chamber. Reagent gas pressures were measured with a Varian 844 ionization gauge. Impulse excitation was used to excite the ions prior to detection.[38−40]

Ion Kinetic Energy Controller. The kinetic energy of ions was controlled by an rf potential on two electrodes radial to the cyclotron motion of the ions. The signal input was provided by a Hewlett-Packard 3325A frequency synthesizer routed through a device to which we refer as the ion kinetic energy controller. The function of the ion kinetic energy controller is described below. The effect of the accelerating signal is to drive ions to progressively larger cyclotron radii and therefore increased kinetic energies.[41,42] Grosshans and Marshall have shown that the resulting radius is overestimated by the infinite electrode approximation,[43−45] and our calculations take this into account. The peak-to-peak voltage of the rf signal used to accelerate the ions was typically in the range of 5−30 V m^{-1}. Acceleration frequencies were kept within 5 Hz of the measured effective cyclotron frequency; the results were fairly insensitive ($\pm 5\%$) to the specific frequency within that 5 Hz range.

The acceleration signal, if applied continuously for even fairly short ($\sim$10 ms) time intervals, would eject resonant ions from the ICR cell, and it would not be possible to observe changes in reactivity that occur on longer (100 ms to 10 s) time scales. To circumvent this problem, the ion kinetic energy controller periodically switches the rf signal so that ions are accelerated for only N cyclotron periods, where N is an integer. At the end of N periods, the phase of the rf signal is reversed by 180°, which drives the ions back to smaller radii and decreased kinetic energies for another N periods of cyclotron motion until the phase of the rf signal is reversed again.[46,47] The ions may be trapped for several seconds, during which time the phase of the rf is reversed at regular intervals. For all of the reactions reported here, the interval between phase shifts was kept at $N = 40$. Because the cyclotron frequency of chloride at 6 kG is approximately 2.5×10^5 Hz, each acceleration or deceleration period lasted roughly 1.6×10^{-4} s.

In the absence of collisions, a particular ion would oscillate between the same minimum and maximum radius indefinitely, where the limiting radii are determined by the vector of ion radial motion at the onset of the driving signal, the rf field strength, and the interval between phase shifts. Collisions serve not only to instantaneously change (and usually lower) the kinetic energy of an ion, but also to displace the maxima and minima of its position function with respect to the phase shifts of the driving signal. For delay times that are long relative to the time scale for collisions, therefore, the steady-state kinetic energy distribution of ions may be determined by summing over the trajectories of ions which undergo a thermalizing collision at a random time in the acceleration/deceleration interval. The resulting kinetic energy distribution, whose form is non-Boltzmann, is calculated with the use of simulations of ion motion rather than analytically. The assumptions of the method and limitations of its use have previously been reported.[48]

RRKM Calculations. We model the reaction kinetics with a double-well potential energy surface such as that shown in Figure 1. The double-well potential has been characterized theoretically and experimentally for a variety of nucleophilic substitution reactions, including those of eqs 2−4.[11,13,14,26,30−35,49−60] We follow closely the methodology used previously in our laboratory to model the kinetics of eq 2,[49] using the RRKM program HYDRA.[61] Details of the modeling may be found in the previous work, but a brief outline is presented here. The overall rate of a reaction is the collision rate of the reactants, k_1 in Figure 1, multiplied by Φ_{tot}, the fraction of total collisions that lead to products.

$$k_{\text{obs}} = k_1 \Phi_{\text{tot}} \tag{5}$$

The rate constant k_{obs} may also be derived from the steady-state approximation as a function of the rate constants in Figure 1:

$$k_{\text{obs}} = \frac{k_1 k_2}{k_{-1} + 2k_2} \tag{6}$$

The variation in the collision rate constant, k_1, as a function of kinetic energy is best computed with classical trajectory calculations, which implicitly account for all of the relevant physics. Su has recently published a parametrized formula that accurately reproduces the results of classical trajectory calculations, and we employ this formula in our calculations.[62] The remaining terms in eq 6 determine the macroscopic efficiency of the reaction, Φ_{tot}, which is the fraction of collisions that lead to reaction.

$$\Phi_{\text{tot}} = \frac{k_2}{k_{-1} + 2k_2} \tag{}$$

The macroscopic efficiency is the sum of its microscopic counterparts, weighted according to the energy and angular momentum distribution of the reactant complex, $F(E,J)$.

$$\Phi_{\text{tot}} = \int \int \Phi(E,J)\, F(E,J)\, \mathrm{d}E\, \mathrm{d}J \tag{7}$$

where each microscopic $\Phi(E,J)$ is the fraction of collisions with energy E and angular momentum J that lead to product formation.

$$\Phi(E,J) = \frac{k_2(E,J)}{k_{-1}(E,J) + 2k_2(E,J)} \tag{8}$$

The individual rate constants, $k(E,J)$, in eq 8 are calculated with unimolecular reaction rate theory, following the μVTST formalism described elsewhere.[49]

(36) Zhong, M.; Brauman, J. I. *J. Am. Chem. Soc.* **1996**, *118*, 636−641.

(37) Wilbur, J. L. Ph.D. Dissertation, Stanford University, 1993.

(38) McIver, R. T.; Hunter, R. L.; Baykut, G. *Anal. Chem.* **1989**, *61*, 489.

(39) McIver, R. T.; Hunter, R. L.; Baykut, G. *Rev. Sci. Instrum.* **1989**, *60*, 400.

(40) McIver, R. T.; Baykut, G.; Hunter, R. L. *Int. J. Mass Spectrom. Ion Proc.* **1989**, *89*, 343.

(41) Beauchamp, J. L. *Annu. Rev. Phys. Chem.* **1971**, *22*, 527.

(42) Freiser, B. S.; Farrar, J. M.; Saunders: W. H. J. *Techniques for the Study of Ion−Molecule Reactions*; Wiley-Interscience: New York, 1988; pp Chapter 2.

(43) Grosshans, P. B.; Marshall, A. G. *Int. J. Mass Spectrom. Ion Proc.* **1990**, *100*, 347−379.

(44) Grosshans, P. B.; Marshall, A. G. *Int. J. Mass Spectrom. Ion Proc.* **1992**, *115*, 1−19.

(45) Grosshans, P. B.; Shields, P. J.; Marshall, A. G. *J. Am. Chem. Soc.* **1990**, *112*, 1275.

(46) Boering, K. A.; Rolfe, J.; Brauman, J. I. *Rapid Commun. Mass Spectrom.* **1992**, *6*, 303−305.

(47) Boering, K. A.; Rolfe, J.; Brauman, J. I. *Int. J. Mass Spectrom. Ion Proc.* **1992**, *117*, 357−386.

(48) Craig, S. L.; Brauman, J. I. *J. Phys. Chem. A* **1997**, *101*, 4745−4752.

(49) Wladkowski, B. D.; Lim, K. F.; Allen, W. D.; Brauman, J. I. *J. Am. Chem. Soc.* **1992**, *114*, 9136−9153.

(50) Brauman, J. I. *J. Mass Spectrom.* **1995**, *30*, 1649−1651.

(51) Lieder, C. A.; Brauman, J. I. *J. Am. Chem. Soc.* **1974**, *96*, 4030.

(52) Brauman, J. I.; Olmstead, W. N.; Lieder, C. A. *J. Am. Chem. Soc.* **1974**, *96*, 4030−4031.

(53) Olmstead, W. N.; Brauman, J. I. *J. Am. Chem. Soc.* **1977**, *99*, 4219.

(54) Asubiojo, O. I.; Brauman, J. I. *J. Am. Chem. Soc.* **1979**, *101*, 3715.

(55) Pellerite, M. J.; Brauman, J. I. *J. Am. Chem. Soc.* **1980**, *102*, 5993.

(56) Dedieu, A.; Veillard, A. *Chem. Phys. Lett.* **1970**, *5*, 328.

(57) Dedieu, A.; Veillard, A. *J. Am. Chem. Soc.* **1972**, *94*, 6730.

(58) Wolfe, S.; Mitchell, D. J.; Schlegel, H. B. *J. Am. Chem. Soc.* **1981**, *103*, 7694.

(59) Tucker, S. C.; Truhlar, D. G. *J. Am. Chem. Soc.* **1990**, *112*, 3338−3347.

(60) Shi, Z.; Boyd, R. *J. Am. Chem. Soc.* **1990**, *112*, 6789.

(61) Wladkowski, B. D.; Lim, K. F.; Brauman, J. I. *HYDRA: Calculation of ion−molecule reaction rate coefficients using variational transition state theory*; 1991.

(62) Su, T. *J. Chem. Phys.* **1994**, *100*, 4703.

$$k(E,J) = \sigma \frac{W_{\mu\text{VTST}}^{\dagger}[\epsilon(J;R^*)]}{h\rho[\epsilon(J;R_e)]} \qquad (9)$$

where σ is the reaction path degeneracy, R denotes the reaction coordinate, $\epsilon(J;R) = E - V(R) - E_r(J;R)$, $W_{\mu\text{VTST}}[E,J]$ is the number of accessible states at the transition state (located at $R = R^*$) for the (E,J) channel, and $\rho[\epsilon(J;R_e)]$ is the corresponding density of states for the ion−molecule reactant complex, whose geometry is given by $R = R_e$. The functions $V(R)$ and $E_r(J;R)$ are the potential energy and the orbital rotational energy, respectively. The choice of reaction path and form of $V(R)$ are determined in a manner similar to that described in previous work.[49] The barrier height obtained to match the thermal rate constant depends slightly on the choice of reaction path and functional form of $V(R)$, and the calculated translational energy dependences (described below) are slightly sensitive to the ultimate choices.

An important consideration in the statistical modeling is the conservation of angular momentum. Because ion−molecule collisions typically have large impact parameters, the total angular momentum (**J**) of the system is dominated by the orbital angular momentum (**L**) of the reactants. It is reasonable, therefore, to make the approximation that **J** = **L**. In this limit, the energy tied up in rotational energy is equal to the orbital rotational energy, $E_r(J;R)$, which is related to the orbital angular momentum through the effective rotational constant for orbital motion, $B(R)$, and the rotational constant for internal rotation of the complex, $A(R)$.

$$E_r(J;R) = B(R) J(J+1) + (A(R) - B(R))\mathbf{K}^2 \qquad (10)$$

We treat **K** as a good quantum number, so that only the first term in the right side of eq 10 needs to be considered. Although this approximation is quite reasonable for thermal ion−molecule systems,[5,19,63] it may introduce error into the RRKM calculations for systems with larger total angular momenta.[19]

As the relative translational energy of the reactants increases, the total energy E and total angular momentum **J** of the reactants will tend toward higher values, altering the distribution $F(E,J)$ in eq 7. The RRKM form of $F(E,J)$ assumes a thermal equilibrium of separated reactants at temperature T,

$$F(E,J) =$$
$$\frac{(2J+1)W_{\mu\text{VTST}}^{\dagger}[E - V_{\text{eff}}(J;R^*)] \exp\left\{\dfrac{-(E - V_{\text{eff}}(J;R^*))}{k_B T}\right\}}{\displaystyle\int\int (2J+1)W_{\mu\text{VTST}}^{\dagger}[E - V_{\text{eff}}(J;R^*)] \exp\left\{\dfrac{-(E - V_{\text{eff}}(J;R^*))}{k_B T}\right\} dE\, dJ} \qquad (11)$$

At increased collision energies, we modify the RRKM calculations as follows. First, the temperature T is replaced with an effective temperature T_{eff}. T_{eff} is chosen so that the average total energy of the system at T_{eff}, calculated in the usual manner from vibrational frequencies obtained in semiempirical calculations, is equal to the average total energy of the reactants at ambient temperature, $T = 350$ K, plus their center-of-mass collision energy.

The angular momentum distribution, and therefore the energy tied up in orbital rotational energy, also increases with kinetic energy. Classically, the orbital angular momentum is proportional to both the relative velocity of the reactants and their impact parameter, b. As the velocity increases, however, the reaction cross section decreases and so does the maximum allowed impact parameter b_{max}. We calculate the collision cross section at a particular collision energy from the value of k_1 determined from Su's formula:

$$\sigma = \frac{k_1}{v} \propto \frac{k_1}{(\text{KE})^{1/2}} \qquad (12)$$

Following Wang and Hase, we assume that the probability of a collision occurring with impact parameter b is proportional to b up to a maximum impact parameter b_{max}, and zero for $b > b_{\text{max}}$.[19] It follows

that b_{max} is proportional to $\sigma^{1/2}$. Since, in the Langevin limit, σ is inversely proportional to v for ion−molecule capture (k_1 is constant), b_{max} varies with $v^{-1/2}$ (in practice, k_1 decreases as v increases, and we calculate the actual variation in b_{max} from eq 12).

In the classical limit, orbital angular momentum is proportional to $v \times b$. Since b falls off as roughly $v^{-1/2}$ (we use the value calculated from eq 12), the probability of a collision occurring with a given orbital angular momentum is proportional to $v^{1/2}$ or $(\text{KE}_{\text{cm}})^{1/4}$. For a fixed geometry R, the energy fixed as rotational energy is proportional to $(\text{KE}_{\text{cm}})^{1/2}$ through the rotational constant $B(R)$. The rotational energies $E_r(J;R)$ are therefore scaled by $(\text{KE}_{\text{cm}}/\text{KE}_{\text{thermal}})^{1/2}$.

The resulting distributions of total and rotational energies are then incorporated into the μVTST-RRKM formalism and combined with the parametrized collision rate to calculate the rate constant as a function of center-of-mass collision energy, $k(\text{KE})$. For comparison with an experimentally observed rate constant, the KE-dependent rate constant is averaged over $P(\text{KE})$, the distribution of kinetic energies determined for our FT-ICR experiments.

$$k_{\text{obs}} = \frac{\displaystyle\int_{\text{KE}} P(\text{KE})\, k(\text{KE})}{\displaystyle\int_{\text{KE}} P(\text{KE})} \qquad (13)$$

$P(\text{KE})$ is taken from trajectory calculations of ions undergoing reversible rf acceleration, the details of which are presented elsewhere.[48]

Reaction Kinetics. The change in reaction rate with kinetic energy was measured in two ways, when possible. The first means of measuring the relative rate constant is achieved by allowing the system to reach a steady-state isotope ratio under conditions where one isotope is continuously accelerated and the other is not. Consider a generic exchange reaction:

$$^{35}\text{Cl}^- + \text{R}^{37}\text{Cl} \underset{k_b}{\overset{k_f}{\rightleftharpoons}} {}^{37}\text{Cl}^- + \text{R}^{35}\text{Cl}$$
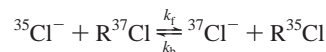
At the steady state,

$$k_f[^{35}\text{Cl}^-][\text{R}^{37}\text{Cl}] = k_b[^{37}\text{Cl}^-][\text{R}^{35}\text{Cl}] >$$

and so

$$\frac{[^{35}\text{Cl}^-]}{[^{37}\text{Cl}^-]} = \frac{k_b[\text{R}^{35}\text{Cl}]}{k_f[\text{R}^{37}\text{Cl}]} \qquad (14)$$

Thus, the steady-state isotope ratio provides a direct measure of the rate constant for the reaction of the accelerated ion relative to that of the thermal ion. We check that the steady state has been achieved by first ejecting one isotope and then the other and seeing that the system relaxes to the same steady-state ratio in both cases. This technique is useful only for those systems that have a high enough rate constant to achieve equilibrium before a significant amount of ion loss has occurred.

In the second type of kinetic experiment, one isotope of chloride ($^{37}\text{Cl}^-$) was isolated and allowed to react with a measured pressure of reagent gas for a fixed period of time. The reaction rate constant describes the rate at which the ion isotope ratio approaches the steady-state isotope ratio.[64]

$$\ln\left[\frac{R_t - R_\infty}{R_t - 1}\right] = -k_{\text{obs}} P t \qquad (15)$$

R_t is the ratio of isotopes at time t, R_∞ is the isotope ratio at equilibrium, and P is the pressure of the neutral reagent. The form of eq 15 takes into account the natural isotope abundance of chloride, so that the pressure P is the total pressure of the neutral reagent. The extent of reaction at a fixed time and pressure is compared for conditions where the reactant isotope is accelerated (subscript "on" in eq 16) with those for which it is not (subscript "off"), and this yields the relative rate constant.

(63) Wang, H.; Hase, W. L. *J. Am. Chem. Soc.* **1997**, *119*, 3093−3102.

(64) Eyler, J. R.; Richardson, D. E. *J. Am. Chem. Soc.* **1985**, *107*, 6130.

$$\frac{\ln\left[\dfrac{R_t^{\text{on}} - R_\infty^{\text{on}}}{R_t^{\text{on}} - 1}\right]_{\text{on}}}{\ln\left[\dfrac{R_t^{\text{off}} - R_\infty^{\text{off}}}{R_t^{\text{off}} - 1}\right]_{\text{off}}} = \frac{k_{\text{on}}}{k_{\text{off}}} = \frac{R_\infty^{\text{on}}}{R_\infty^{\text{off}}} \qquad (16)$$

Note that the steady-state isotope ratio R changes as one isotope is accelerated and the other is not, and the new ratio (and, from eq 14, the relative rate constant) shows up on both sides of eq 16. Equation 16 may be solved to yield the relative rate constant as a function of KE.

The second, "one-way" relative rate measurements were performed for all of the reactions, whereas the first "steady-state" method was only applied to the faster exchange reactions. Excellent agreement ($\pm5\%$) between methods was obtained for all cases in which both methods were applied.

Results and Discussion

Several gas-phase S_N2 reactions, such as those in eq 1, exhibit nonstatistical behavior.[6-14,16-22] The nonstatistical dynamics arise from an apparent bottleneck to T $\leftrightarrow$ V energy transfer. When intermediates in these systems are formed at increased collision energies, the energy remains trapped in intermolecular motions of the ion and neutral reactant rather than sampling the available phase space of the intermediate prior to dissociation or reaction.[20] As a result, the changes in reactivity at increased KE reflect the bottleneck to energy transfer rather than the potential energy surface of the reaction. There is reason to expect that the nonstatistical behavior might be limited to special cases. Equations 1, for example, comprise small systems with fairly low association energies (approximately 10 kcal mol^{-1}), nonstatistical KERDs of product complexes, and nonstatistical reactivity in reactant complexes that involve ion−molecule intermediates which are quite energetic. The expected lifetimes of the intermediates, therefore, are very short and thus limit the extent of energy redistribution.[65]

By studying a series of similar reactions, eqs 2−4, we hope to see whether the observed energy dependences of the reactions are consistent with changes in their potential energy surfaces. The potential energy surfaces of all of these reactions have been studied in our laboratory by measuring the kinetics of chloride exchange at ambient temperatures.[33,49,66] Transition state frequencies were obtained from either ab initio (eq 2) or semiempirical (eqs 3 and 4) calculations, and the central barrier height was adjusted for each reaction to fit the observed thermal rate constant. The observed kinetics and inferred barrier heights are listed in Table 1.
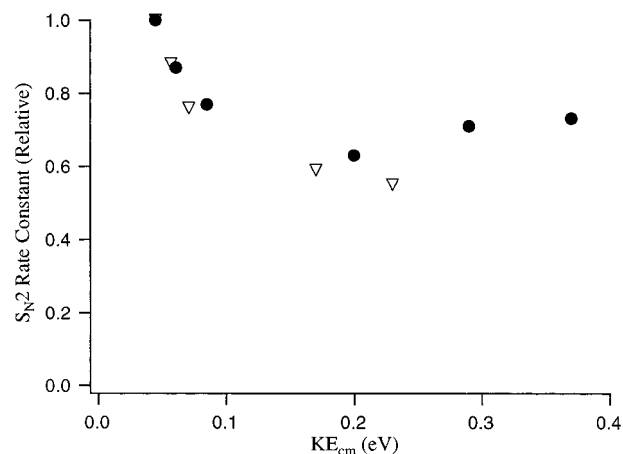
The relative rate constants of the two S_N2 reactions, eqs 2 and 3, are shown in Figure 2. Although these reactions have very different activation energies (−2.6 kcal mol^{-1} for m-FC$_6$H$_4$-CH$_2$Cl, −5.9 kcal mol^{-1} for ClCH$_2$CN), they show similar negative KE dependences at lower translational energies. At lower collision energies, the variation in reaction rate for the slower m-FC$_6$H$_4$CH$_2$Cl reaction ($\Phi = 0.008$) is only slightly less than that of ClCH$_2$CN ($\Phi = 0.11$), until the m-FC$_6$H$_4$CH$_2$-Cl rate begins to increase with KE at around 0.2 eV collision energy.

The overall KE dependence reflects changes in both the collision rate constant (k_{coll}) and the efficiency (Φ_{tot}). The collision rate is calculated from the parameters derived by Su from trajectory calculations,[62] which take into account all of the important physics of the collision event. The change in Φ_{tot}

(65) Boering, K. A.; Brauman, J. I. *J. Chem. Phys.* **1992**, *97*, 5439.
(66) See ref 35.

Table 1. Reaction Rates, Efficiencies, and Activation Energies of Chloride Exchange Reactions ^{37}Cl$^-$ + R^{35}Cl → ^{35}Cl$^-$ + R^{37}Cl

R	k_{obs} $(10^{-10}$ cm^3 s$^{-1})$	k_{coll} $(10^{-9}$ cm^3 s$^{-1})$	Φ	$E_{\text{diff}}{}^a$
m-FC$_6$H$_4$CH$_2$−	0.18^b	2.3^b	0.008^b	−2.6^b
p-CH$_3$C$_6$H$_4$CO−	0.86^c	3.9^c	0.022^c	−4.0^c
m-CH$_3$C$_6$H$_4$CO−	2.7^c	3.6^c	0.074^c	−5.8^c
C$_6$H$_5$CO−	3.4^c	3.5^c	0.097^c	−5.9^c
(CN)CH$_2$−	3.2^d	3.0^d	0.11^d	−5.9^d
m-(F)C$_6$H$_4$CO−	7.9^c	2.8^c	0.28^c	−8.8^c
m-(CF$_3$)C$_6$H$_4$CO−	11.2^c	2.9^c	0.38^c	−11.0^c

^{a} Units: kcal mol^{-1}. ^{b} Reference 33. ^{c} Reference 35. ^{d} Reference 49.

Figure 2. The relative rate constants for S_N2 chloride exchange reactions of ClCH$_2$CN ($\triangledown$) and m-FC$_6$H$_4$CH$_2$Cl ($\bullet$) as a function of average center-of-mass kinetic energy calculated for the reversible acceleration of ions in the FT-ICR. The relative rate constants are reproducible to $\pm10\%$. Absolute rate constants have been reported previously and are given in Table 1.

reflects the effect of KE on the individual rate constants k_{-1} and k_2, which are the processes frequently modeled with statistical theory.

In the statistical limit, the origin of the KE dependence of the rate constants is 2-fold. First, collisions at increasing KE have larger orbital angular momenta, and the energy tied up in angular rotational energy will be much larger for collisions at higher KE. This creates an increased effective barrier to the S_N2 reaction in high-energy collisions. Second, reactions with negative activation energies will have negative overall energy dependences. Each of these factors contributes to the initial decrease in the reaction rate constants with increasing KE.

The KE dependence need not be monotonic, however. Conservation of angular momentum can raise the effective activation energy of the reaction above the energy of separated reactants for high **J** values.[67] When this occurs, the overall energy dependence of the rate constant will become positive. Since the angular momentum barrier will increase as approximately (KE)$^{1/2}$ and the total energy will increase with KE, the variation in reaction rate with KE will level off and may eventually reverse at higher translational energies. Our experimental results for the S_N2 reaction of m-FC$_6$H$_4$CH$_2$Cl indicate that a minimum S_N2 rate constant is obtained at a collision energy of approximately 0.20 eV.

The KE at which a rate constant begins to increase will depend on several factors, most importantly the relative activation energies and rotational constants of the isomerization and dissociation transition states. Wang and Hase have observed

(67) Troe, J. *Int. J. Mass Spectrom. Ion Proc.* **1987**, *80*, 17.
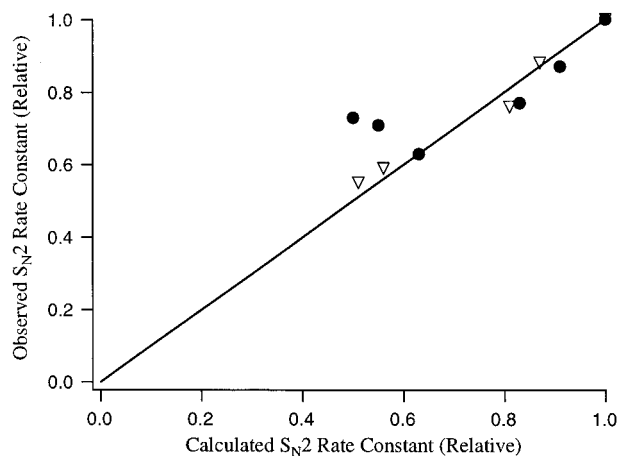
Figure 3. Comparison of the observed S$_N$2 chloride exchange reaction rate constants for ClCH$_2$CN ($\triangledown$) and *m*-FC$_6$H$_4$CH$_2$Cl ($\bullet$) with those expected from RRKM theory (see text for details) at increased center-of-mass kinetic energy. Only the relative rate constants (normalized to their 350 K thermal values) are shown. The relative rate constants are reproducible to ±10%. If agreement between theory and experiment were perfect, the data points would fall along the straight line *y = x*, shown.

Figure 4. The relative rate constants for addition−elimination chloride exchange reactions of XC$_6$H$_4$C(O)Cl (X = *m*-CF$_3$ (×), *m*-F (△), H (+), *m*-CH$_3$ ($\bullet$), *p*-CH$_3$ ($\bigcirc$)) as a function of average center-of-mass kinetic energy calculated for the reversible acceleration of ions in the FT-ICR. The relative rate constants are reproducible to ±10%. Absolute rate constants have been determined elsewhere and are given in Table 1.

such a turning point in their rigorous RRKM calculations for reaction 1b.[68] The exact collision energy of the minimum rate constant depends on the choice of ΔE_{diff}. When ΔE_{diff} is −1.7 kcal mol^{-1}, the turning point occurs at around 0.13−0.15 eV, while ΔE_{diff} = −3.0 kcal mol^{-1} corresponds to a turning point at 0.21−0.23 eV. These values are very consistent with the observed behavior in the S$_N$2 reaction of *m*-FC$_6$H$_4$CH$_2$Cl, which has a calculated ΔE_{diff} of −2.6 kcal mol^{-1} and a minimum rate constant at a collision energy of approximately 0.20 eV.
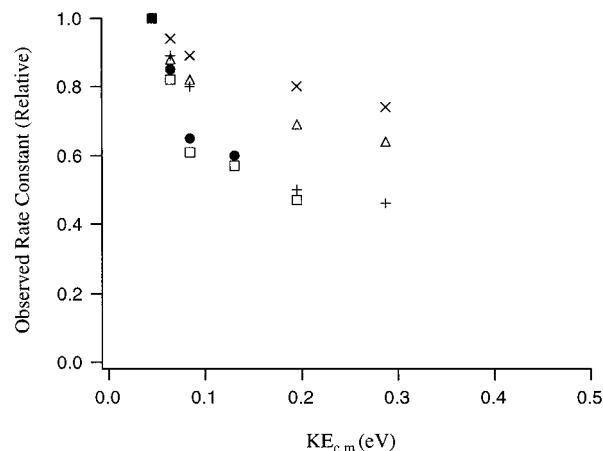
The upturn in the KE dependence could, in theory, be due to the opening of a new channel for chloride exchange, but this is unlikely for eq 3 for several reasons. First, there are no additional reactions, such as elimination, that are accessible at these energies. Second, the upturn is not observed in eqs 1b, 2, or 4, and although direct displacement at increased KE has been implicated in eq 1a,[24,69] the threshold energy is much higher than observed here and the cross sections are considerably lower. Finally, the upturn agrees with Wang and Hase's detailed calculations for 1b.

An RRKM analysis of the reaction conditions yields very similar KE dependences for eqs 2 and 3, in good agreement with the experimental observations. As seen in Figure 3, the experimental data and RRKM results are in good quantitative agreement, with the exception of the higher energy data for the *m*-FC$_6$H$_4$CH$_2$Cl exchange reaction. Our RRKM calculations do not reproduce the observed reversal in the KE dependence. This may be a consequence of our treatment of angular momentum, in which we assume that the inactive external rotor is uncoupled to the internal rotations of the neutral reactant. As a consequence, the increased orbital angular momentum is modeled as residing entirely in the external rotor; **K** is treated as a good quantum number. While our model is likely to be reasonable,[19,49,63] Wang and Hase have recently pointed out that a more thorough consideration of angular momentum may be necessary at large relative translational energies.[70] Nevertheless, the observation of an increasing reaction rate with KE is strong evidence that energy is redistributed in high-energy collisions.

The absolute magnitudes of the KE dependences are also significant, primarily because they are much smaller than that observed for eq 1b. While the relative rate constant of eq 1b at 0.08 eV center-of-mass collision energy is roughly 50% of the thermal value, the relative rate constant of chloride exchange in *m*-FC$_6$H$_4$CH$_2$Cl has decreased only about 25% at the same energy. The activation energies and efficiencies of the two reactions are very similar, and yet the variation with KE in eq 1b is roughly twice that of eq 3. The KE dependence of the latter reaction is in line with our RRKM analysis of that reaction, and it is very similar to the RRKM calculations of Wang and Hase for eq 1b. Thus, it is unlikely that the inability of statistical theories to model eq 1b is due either to errors in the potential energy surfaces or to inadequacies in the calculations. Rather, the dynamics of eq 1b are fundamentally different from those of eq 3.

In addition to the S$_N$2 reactions cited above, we have also studied the KE dependences of the carbonyl addition−elimination (AE) reactions in eq 4. In this series, the variation in the observed rate constant with KE is quite sensitive to the reactant, although the rates of all of the AE exchange reactions, shown in Figure 4, decrease monotonically with increasing KE across the range examined. For this series, the slower reactions have greater KE dependences. Because one might expect that T ↔ V coupling would be the same for this series of very similar reactions, the observation of differential KE dependences suggests that the energy dependence reflects the features of the reaction potential energy surfaces, such as the activation energy, which do change.

Figure 5 shows that the trend in reactivity is consistent with an RRKM analysis, as the expected energy dependences are also greatest for the slowest reactions. The progression in the KE dependences is easily understood from the potential energy surfaces of the reactions. High reaction efficiencies correspond to low activation energies. As the barrier to reaction becomes smaller, the potential energy surface approaches the limit of a barrierless single-well surface. In this limit, a reaction occurs with every collision (or 50% of all collisions for thermoneutral reactions such as eqs 2−4), and the overall energy dependence of the reaction would reflect only the variation in the collision rate (see Figure 6).

(68) Wang, H.; Hase, W. L. Personal communication.

(69) Mann, D. J.; Hase, W. L. *Abstracts, 215th ACS National Meeting of the American Chemical Society, Dallas,* March 29−April 2, 1998; American Chemical Society: Washington, DC; PHYS-121.

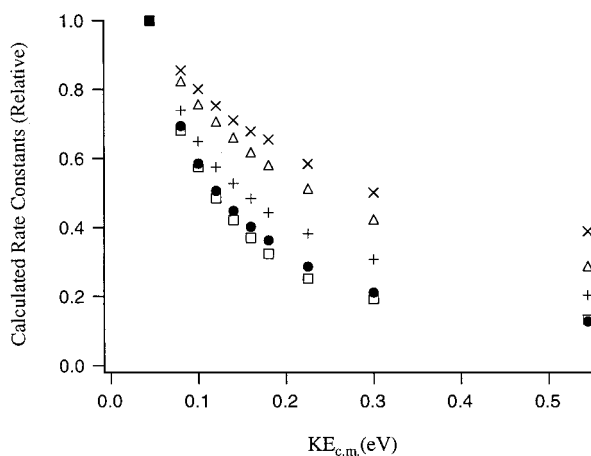(70) Wang, H.; Hase, W. L. *Chem. Phys.* **1996,** *212,* 247−258.

Figure 5. The calculated relative rate constants for addition−elimination chloride exchange reactions of $XC_6H_4C(O)Cl$ (X = m-CF_3 (×), m-F (△), H (+), m-CH_3 (●), p-CH_3 (○)) as a function of center-of-mass kinetic energy. Calculations are based upon potential energy surfaces for the reactions, which have been determined elsewhere. Activation energies are given in Table 1.
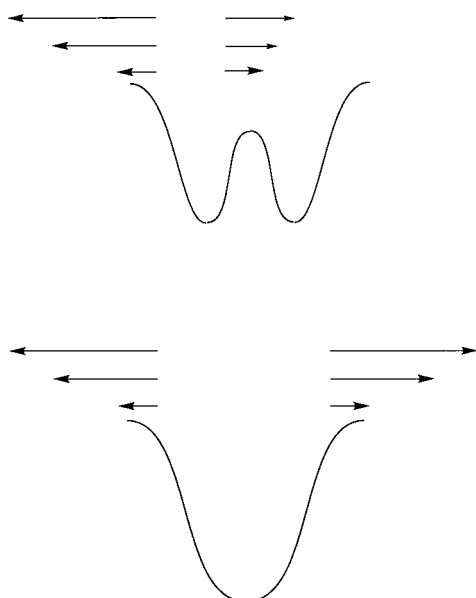
Figure 6. Comparison of the energy dependence of a double-well vs single-well symmetrical potential energy surface. Reactions on a double-well surface with a negative activation energy will exhibit a negative energy dependence, due to competition between the central barrier and dissociation pathway. In the barrierless single-well surface, however, the reaction efficiency is determined by competition between the two dissociating pathways, which have identical energy dependences. Thus, as reactions become faster due to lower activation energies, the reaction efficiencies will have progressively less energy dependence. By comparison, reactions with activation energies at the entrance channel should exhibit little energy dependence, and those with positive activation energies should exhibit a positive energy dependence.

The expected RRKM rate constants may again be calculated by summing the RRKM rates over the appropriate distribution of kinetic energies, and comparing the calculations to the experimental results. As seen for the S_N2 reactions, the overall agreement between experiment and theory for the AE reactions is quite good (Figure 7). Some deviation from the calculated values is observed, primarily for the reactions of m-$(CF_3)C_6H_4C$-(O)Cl, m-$(CH_3)C_6H_4C(O)Cl$, and p-$(CH_3)C_6H_4C(O)Cl$. These reactions possess activation energies that are either far below (m-$(CF_3)C_6H_4C(O)Cl$) or fairly close to (m-$(CH_3)C_6H_4C(O)Cl$)
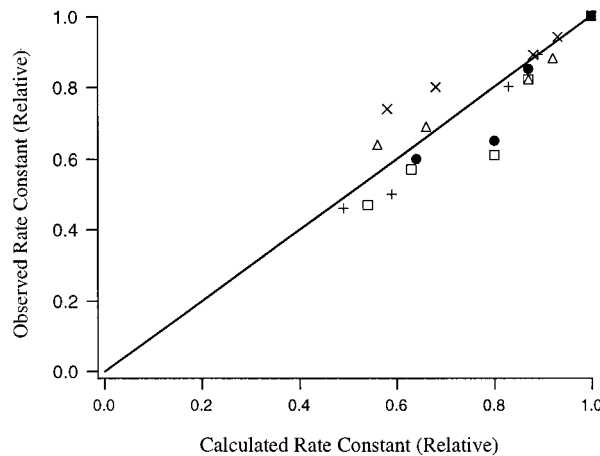
Figure 7. Comparison of the observed S_N2 chloride exchange reaction rate constants for $XC_6H_4C(O)Cl$ (X = m-CF_3 (×), m-F (△), H (+), m-CH_3 (●), p-CH_3 (○)) with those expected from RRKM theory (see text for details) at increased center-of-mass kinetic energy. Only the relative rate constants (normalized to their 350 K thermal values) are shown. The relative rate constants are reproducible to ±10%. If agreement between theory and experiment were perfect, the data points would fall along the straight line $y = x$, shown.

and p-$(CH_3)C_6H_4C(O)Cl$ the entrance channel. For these potential energy surfaces, uncertainty in the exact rate constant measurement and calculated vibrational frequencies leads to greater uncertainty in the derived value of ΔE_{diff} than for reactions with intermediate efficiencies.[71] Because the calculated KE dependence is quite sensitive to ΔE_{diff}, the disagreement between the calculations and the experimental results more likely reflects a propagation of uncertainties from various aspects of the work rather than a breakdown in the underlying assumptions of the theory.

The observed energy dependences of the reactions in eqs 3 and 4, then, are consistent with a statistical model in which T ↔ V energy redistribution is assumed to be efficient and the increased translational energy of the reactants samples the entire potential energy surface of the reaction. The behavior of these reactions is similar to that observed for eq 2,[28,29] and provides greater support for the general validity of RRKM and related theories as a means of interpreting not only the thermal rate constants of bimolecular ion−molecule reactions, but also their kinetic energy dependences.

Hase has proposed that the dynamics of S_N2 reactions can be interpreted in terms of the scheme in Figure 8.[20] Ion−molecule capture occurs at the collision rate to generate an "intermolecular" reactant complex. This complex is formed by T → R energy transfer, and that energy is initially unavailable to the reaction coordinate. Energy then flows into the vibrational modes of the neutral reactant to form an "intramolecular" reactant complex, in which the redistributed energy is now available for reaction. If energy flow is slow on the time scale for dissociation, the intermolecular complexes will dissociate before the microcanonical ensemble is established and reactivity will be below the statistical expectation. The relative rates of dissociation and energy transfer determine the validity of the statistical theory.

Although the detailed reaction dynamics are surely more complex than this simple model, the expected lifetimes provide

(71) The absolute rate measurements are only accurate to ±30% due to uncertainties in the total pressure measurements. For the fastest reaction in eq 4, the efficiency of 0.38 could be from 0.26 to 0.50, corresponding to activation energies in the range −8.7 kcal/mol to barrierless (−18 kcal/mol). A 30% variation in an efficiency of 0.10, however, only corresponds to an uncertainty in activation energy of around ±1 kcal/mol.
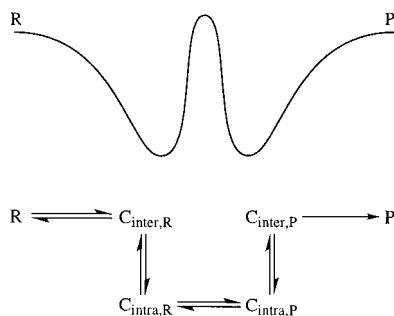
Figure 8. Dynamical model for the S$_N$2 reaction proposed by Hase.[20] The reactants, R, intially come together to form a reactant complex with energy in its intermolecular modes ($C_{inter,R}$). For reaction to occur, energy must transfer into the intramolecular modes of the complex to generate $C_{intra,P}$. If dissociation is fast relative to energy redistribution, the observed reaction rate constant will be less than the statistical expectation, especially in intermediates formed at elevated collision energies.

a convenient explanation of the observed behavior in eqs 1−4. Unlike the collision complexes in eq 1, which have lifetimes on the order of 10−100 ps,[26] we calculate that the RRKM lifetimes of the intermediates in eqs 2−4 are on the order of 10 ns or greater at the energies accessed in these experiments. These intermediates appear to live long enough for energy to redistribute statistically. The microcanonical ensemble, therefore, is maintained, and statistical theories describe the KE dependences of these reactions quite well. Morris and Viggiano have reported that the S$_N$2 reactions F$^-$ + CF$_3$X (X = Cl, Br, I) show statistical behavior, and the observation of association channels suggests that the lifetimes of the intermediate complexes are long enough for energy redistribution.[17,72]

As with the nonstatistical KE dependences, the nonstatistical KERD's observed by Graul and Bowers might also reflect competition between unimolecular decomposition and energy transfer. In eq 1b, for example, the S$_N$2 product complex is initially intramolecularly excited, and energy must redistribute into intermolecular modes for dissociation to occur. Energy redistribution into the intermolecular modes will occur until the rate of dissociation is comparable to the rate of energy redistribution. Given the short lifetimes of the structurally similar

intermediates in eq 1a, it is reasonable to expect that the dissociation rate will become very fast with only a small amount of energy redistributed into the intermolecular modes. Dissociation of the product complex might easily occur before the microcanonical energy distribution has achieved the statistical ensemble, resulting in a KERD that is below the statistical expectation.

The conversion from intermolecular to intramolecular complexes has been estimated to take place on time scales on the order of tenths of picosecond, and the time necessary for energy in a system such as eq 1 to be fully randomized will be in the 1 to 10 ps range.[68] It is therefore not surprising, given their expected lifetimes, that eqs 2−4 behave statistically. As the total energy of the system increases, the lifetime will decrease and systems that behave statistically at thermal energies will exhibit nonstatistical character. Such a transition has been observed to enhance the reactivity of a vibrationally activated intermediate,[27] and a similar transition is expected for intermolecularly excited species. Incomplete energy transfer will likely become important for intermediates with lifetimes shorter than 100 ps, and further experimental and theoretical studies of such species should provide more insights into the dynamics of ion−molecule reactions.

Conclusions

The kinetic energy dependences of an S$_N$2 and several addition−elimination chloride exchange reactions have been reported. The rate constants vary with increasing kinetic energy in a manner that is qualitatively and quantitatively consistent with an RRKM analysis. The agreement between theory and experiment in these reactions supports the assertion that the underlying assumptions of statistical unimolecular reaction rate theory, particularly that of rapid energy randomization, should be valid for long-lived ion−molecule intermediates.

(72) Morris, R. A.; Viggiano, A. A. *J. Phys. Chem.* **1994**, *98*, 3740.